The Open Medicinal Chemistry Journal
DOI: 10.2174/0118741045448792260324171418, 2026, 20, e18741045448792
ISSN: 1874-1045

RESEARCH ARTICLE OPEN ACCESS

Targeting WEE1 Kinase with Phytochemicals from *Ampelocissus thyrsiflora* (Blume) Planch: An Integrated *In Silico* and *In Vitro* Study Against Human Breast Cancer Cells

Henny Sri Wahyuni[1,*], Sri Yuliasmi[2], Nazliniwaty[3], Nilsya Febrika Zebua[4], Gracelyn Tanaka[5], Pinastiara Br Napitupulu[5] and Clara Claudia Jap[1]

[1]*Department of Pharmaceutical Chemistry, Faculty of Pharmacy, Universitas Sumatera Utara, Medan 20155, Indonesia*
[2]*Department of Pharmaceutical Chemistry, Faculty of Vocational Studies, Universitas Sumatera Utara, Medan, 20155, Indonesia*
[3]*Department of Pharmaceutical Technology, Faculty of Pharmacy, Universitas Sumatera Utara, Medan 20155, Indonesia*
[4]*Department of Pharmaceutical Chemistry, Faculty of Pharmacy, Universitas Tjut Nyak Dhien, Medan, 20123, Indonesia*
[5]*Undergraduate Program, Faculty of Pharmacy, Universitas Sumatera Utara, Medan 20155, Indonesia*

Abstract:

Introduction: Breast cancer is the second most diagnosed cancer worldwide, with WEE1 kinase recognized as a key regulator of tumor progression. Natural products, particularly plant-derived metabolites, offer promising scaffolds for the development of novel WEE1 inhibitors.

Materials and Methods: Ethanol extracts of *Ampelocissus thyrsiflora* (Blume) Planch, a North Sumatran endemic plant, were obtained *via* maceration and subjected to phytochemical screening, PASS prediction, and Lipinski's Rule of Five evaluation. Molecular docking and 100 ns molecular dynamics (MD) simulations were performed to investigate ligand–protein interactions. Cytotoxicity was assessed using the MTT assay on MCF-7 breast cancer cells.

Results: Phytochemical analysis confirmed the presence of alkaloids, flavonoids, saponins, tannins, glycosides, and steroids. Fourteen compounds exhibited strong predicted biological activity, and thirteen fulfilled drug-likeness criteria. Based on binding affinity and interactions with key WEE1 residues, four compounds were selected for MD simulations. Three demonstrated favorable MM-PBSA binding energies and stable interactions with critical residues. The ethanol extract showed an IC_{50} of 2011.25 ± 42.71 µg/mL against MCF-7 cells.

Discussion: The computational results highlight the potential of *A. thyrsiflora* metabolites as multi-target inhibitors of WEE1 kinase. Although the obtained IC_{50} value is comparatively high, the result provides an important preliminary basis for subsequent investigations and potential optimization of its active constituents.

Conclusion: Although the ethanol extract of *A. thyrsiflora* exhibited a high *in vitro* IC50, the *in silico* results provide a strong rationale for further exploration of its metabolites as potential WEE1-targeted anticancer agents.

Keywords: *Ampelocissus thyrsiflora*, Molecular docking, Molecular dynamics, Cytotoxicity assay, MTT assay, MCF-7.

*Address correspondence to this author at the Department of Pharmaceutical Chemistry, Faculty of Pharmacy, Universitas Sumatera Utara, Medan 20155, Indonesia; Tel: +628126217358; E-mail: henny@usu.ac.id

Cite as: Wahyuni H, Yuliasmi S, Nazliniwaty , Zebua N, Tanaka G, Napitupulu P, Jap C. Targeting WEE1 Kinase with Phytochemicals from *Ampelocissus thyrsiflora* (Blume) Planch: An Integrated *In Silico* and *In Vitro* Study Against Human Breast Cancer Cells. Open Med Chem J, 2026; 20: e18741045448792.
http://dx.doi.org/10.2174/0118741045448792260324171418

Received: October 17, 2025
Revised: December 14, 2025
Accepted: January 05, 2026
Published: March 27, 2026

1. INTRODUCTION

Cancer is a deadly disease that arises from genetic alterations in cells, leading to uncontrolled proliferation and tumour development [1]. According to GCO data, breast cancer is the second most frequently diagnosed malignancy, accounting for more than 11.6% of all cancers in women [2, 3]. Among the critical regulators of cell cycle progression is WEE1 protein kinase, which negatively regulates CDK1 and enforces the G2/M checkpoint, allowing cells time to repair DNA damage before mitosis. However, in cancer cells, this checkpoint is often exploited as a survival mechanism, enabling damaged and genetically unstable cells to persist [4, 5]. Targeting WEE1 has thus emerged as an urgent therapeutic strategy, as its inhibition can abrogate the G2 arrest, forcing DNA-damaged cells to prematurely enter mitosis and undergo apoptosis. This mechanism not only accelerates cell death but also sensitizes tumor cells to DNA-damaging chemotherapies and radiotherapy. The development of selective WEE1 inhibitors is therefore a high-priority area in cancer research, as they offer a more effective anti-tumor response compared to non-selective agents [6-8].

Adavosertib is a highly selective WEE1 inhibitor that increases tumor cell sensitivity to chemotherapeutic agents and replication stress [9, 10]. However, chemotherapy-based treatments are often associated with severe side effects such as nephrotoxicity, hepatotoxicity, and cardiotoxicity, and can also damage healthy DNA [11]. Consequently, there is a need for new, more targeted therapies with fewer side effects, such as those derived from natural metabolite compounds for the inhibition of cancer cell growth.

Ampelocissus thyrsiflora (Blume) Planch is a typical North Sumatran plant widely used in traditional medicine by the Karo people [12]. Phytochemical studies have shown that *A. thyrsiflora* contains various bioactive compounds, including alkaloids, flavonoids, saponins, tannins, and glycosides, which possess antioxidant and anticancer properties. Previous studies have also demonstrated its potent antioxidant activity and therapeutic benefits in tissue repair, reduction of lung inflammation, and hepatoprotection [13-15]. Additionally, toxicity screening using the Brine Shrimp Lethality Test (BSLT) revealed cytotoxicity, with an LC_{50} of 187.086 ppm against *Artemia salina* Leach, indicating that the plant contains compounds with bioactivity worth exploring [16].

Building on these findings, *A. thyrsiflora* has previously been reported to exhibit activity against SIRT1 and AMPK, which are associated with anticancer pathways [17]. Quercetin, a secondary metabolite contained in *A. thyrsiflora,* was known to suppress WEE1 expression *in vitro,* while isorhamnetin also effectively downregulated WEE1 expression [18, 19]. This suggests its potential as a WEE1 inhibitor. Molecular docking is a predictive, cost-effective method for identifying molecular interactions between plant-derived compounds and target proteins by evaluating binding affinity and stability. This technique facilitates the early-stage discovery of promising drug candidates [20]. Given this context, we conducted an experimental study integrating computational and *in vitro* assays to identify potential WEE1-targeting compounds from *A. thyrsiflora* leaves. These findings may contribute to new insights into the therapeutic potential of this underexplored plant species in breast cancer treatment.

2. MATERIALS AND METHODS

2.1. Materials

The materials used include a computer with ASUS ROG Zenith II Extreme Alpha, AMD Ryzen Threadripper 3970X, NVIDIA GeForce RTX 4090, AutoDock Vina, PyMOL, Biovia Discovery Studio [21], GROMACS, g-mmpbsa, PASS Online website (http://way2drug.com/PassOnline/), Lipinski's Rule of Five websites (https://www.scfbioiitd.res.in/software/drugdesign/lipinski.jsp), pkCSM Online Tools website (https://biosig.lab.uq.edu.au/pkcsm/), CHARMM-GUI (https://www.charmm-gui.org/), PROTOX-II website (https://tox.charite.de/protox3/), Protein Data Bank website (https://rcsb.org/), and PubChem website (https://pubchem.ncbi.nlm.nih.gov/).

2.2. Methods

This study employed an experimental, exploratory design to evaluate the interaction between phytochemicals from *Ampelocissus thyrsiflora* and the WEE1 kinase using *in silico* approaches and *in vitro* cytotoxicity assays. The study involved phytochemical characterization, molecular docking, molecular dynamics simulations, and MTT assay on MCF-7 cells. The primary variables assessed included binding energy, interaction residues, and IC_{50} values.

2.3. Extraction of *A. thyrsiflora* Leaves

Plant identification was carried out at the Badan Riset dan Inovasi Nasional (BRIN) under the reference number

B-3283/II.6.2/IR.01.02/9/2024. The extraction process was carried out using 5 liters of 96% ethanol as the solvent for 500 grams of powdered *A. thyrsiflora*. The maceration was conducted at room temperature for 3 × 24 hours with stirring every 8 hours. The extract was filtered using filter paper to separate the filtrate from the residue. The filtrate was then concentrated using a rotary evaporator to obtain a thick extract. The yield of the extract was subsequently calculated [22, 23].

2.4. Phytochemical Screening of Ethanol Extract of *A. thyrsiflora* Leaves

Phytochemical screening of the ethanol extract of *A. thyrsiflora* leaves was conducted to detect the presence of secondary metabolites, including alkaloids, flavonoids, saponins, tannins, glycosides, and steroids. Alkaloids were identified using Mayer's, Dragendorff's, and Bouchardat's reagents [24]. Flavonoids were detected by mixing the ethanol-dissolved extract with concentrated HCl and magnesium. Saponins were confirmed by the formation of stable foam. Tannins were identified upon the addition of 0.1% ferric chloride. Glycosides were detected by the treatment with NaOH [25], while steroids were confirmed through the Liebermann–Burchard test [26].

2.5. Chemical Compounds

Based on LC-HRMS analysis, 39 secondary metabolite compounds were identified in the ethanol extract of *A. thyrsiflora*, consisting of: Valproic Acid; Phenyl salicylate; Ribonic acid; Ethylparaben; 3',4'-dimethoxy-alpha-naphthoflavone; 6,6,9-trimethyl-3-(3-methyloctan-2-yl)-7,8,9,10 tetra hydrobenzo[c]chromen-1-ol;Dipropyleneglycol methyl ether acetate; Arbutin; 5-[6-hydroxy-5-(3-methylbut-2-enyl)-1-benzofuran-2-yl] benzene-1,3-diol; Lauric acid; 4,4-Dimethyl-5 alpha-cholesta-8,14,24-trien-3 beta-ol; Norethindrone acetate; 2, 4, 5-trihydroxy-7, 8-dioxonaphthalen-1-olate; (2S,3S)-2,3-Dihydro-2-[2-hydroxy -4-(betaDglucopyranosyloxy) phenyl]-3-(3, 5-dihydroxy-phenyl) -4-[2-[4-(beta-D-glucopyranosy loxy) phenyl] ethenyl]benzofuran-6-ol; 3-hydroxy-3 methyl butanoate; Acetic acid; 1-Naphthylbis (9-anthryl) methylcation; 4-phenylethynylnaphthalic anhydride; [(2S,3R,4S,5S,6R)-3,4,5-trihydroxy-6-[[(2R,3R,4R,5R,6S)-3,4,5-trihydroxy-6-methyloxan-2-yl]oxymethyl]oxan-2-yl] (E)-3-phenylprop-2-enoate; ethane; (13Z, 16Z)-docosa-13, 16-dienoic acid; Carthamoleusterone; 5-propan-2-yl-1, 3-benzodioxole; 3-[(2-carboxyacetyl) oxymethoxy]-3-oxopropanoic acid; Myricetin; Mearnsitrin; Quercetin; Kaempferol; 5,8-dihydroxy-2-(4-hydroxyphenyl)-7-methoxy-3-{[(2S,3R,4R,5R,6S)-3,4,5-trihydroxy-6-methyloxan-2-yl]oxy}-4H-chromen-4-one; Isorhamnetin; Oleamide; Hexadecanamide; Stearamide; 1-Stearoylglycerol; Tridemorph; Erucamide; Bis(2-ethylhexyl) phthalate; Stearic acid; DL-α-Tocopherol.

2.6. Preparation of the Biology Activity Prediction

SMILES were first retrieved from PubChem and submitted to the PASS Online. Activating the prediction would show all the results [27].

2.7. Preparation of Physicochemical Prediction

All compounds were saved in pdb format from PubChem and subjected to Lipinski's Rule of Five. On the web, the 3D structures in pdb format should be submitted after the pH is set to 7 [28].

2.8. Molecular Docking

Docking was performed using AutoDock Vina with the 3D structure of the WEE1 receptor (PDB ID: 5VC5), while a total of 39 compounds from *A. thyrsiflora* obtained from PubChem were docked, and the docking process was conducted twice. The receptor was separated from the native ligands and water molecules, polar hydrogens were added, and Gasteiger charges were computed. Furthermore, a 30 × 30 × 30 Å grid box was used in the docking process [29, 30]. After obtaining the docking results, the lowest binding affinity was selected. Pymol software was used to examine the RMSD value. Visualization of the docking results was then performed using Biovia Discovery Studio [31]. Data were analyzed using IBM SPSS Statistics, and the mean ± standard deviation (SD) value.

2.9. Molecular Dynamics Simulations

Molecular dynamics (MD) simulations were generated from docking output and subsequently refined with CHARMM-GUI (https://www.charmm-gui.org/) to produce the topology files required for the MD simulations. The GROMACS force field was applied to define the systems and ligand parameters. The system temperature was maintained at 310°K throughout the simulation [32]. The simulations were executed using GROMACS 2022.4. An initial energy minimization was conducted to stabilize the system. The production phase involved a 100 ns simulation with a 4 fs time increment. Various metrics were analyzed, such as RMSD, RMSF, SASA, hydrogen bonding, and MMPBSA, and the results were visualized with GMXTools and g-mmpbsa [33, 34]. Data were analyzed using IBM SPSS Statistics, and the mean ± standard deviation (SD) value.

2.10. Ethics Approval

This study was conducted in accordance with the principles of the Declaration of Helsinki. Ethical approval was obtained from the Animal Research Ethics Committee of the Faculty of Mathematics and Natural Sciences, Universitas Sumatera Utara, Indonesia (Approval No. 0950/KEPH-FMIPA/2024). All experimental procedures were performed in compliance with institutional ethical guidelines.

2.11. Cytotoxicity Assay

MCF-7 cells (ATCC, HTB-22), were obtained from the Laboratory of Parasitology, Faculty of Medicine, Public Health, and Nursing, Universitas Gadjah Mada, Indonesia. The cells were seeded in 96-well plates at a density of 1×10^4 cells/100 µL and incubated for 24 hours in a CO_2 incubator at 37 °C. The ethanol extract of *A. thyrsiflora* leaves and adavosertib, dissolved in DMSO, were then

added to the medium at concentrations of 1000, 500, 250, 125, and 62.5 µg/mL, with three replicates per concentration. After 24 hours of incubation, the medium was removed, and 100 µL of 0.5 mg/mL MTT solution was added to each well. After 6 hours, 10% SDS was added. The optical density (OD) was measured using a microplate reader at 595 nm [35, 36].

3. RESULTS AND DISCUSSION

3.1. Ethanol Extract of *A. thyrsiflora* Leaves

The extraction of *A. thyrsiflora* was carried out using 96% ethanol. This choice was based on the characteristics of 96% ethanol, which can extract both polar and non-polar compounds, as well as the advantages of the maceration method, which is easy to perform and does not require heating, thus preventing the degradation of the compounds present in the sample [37]. The extraction yielded a concentrated extract of 95.91 grams [38]. The extract yield was then calculated by comparing the final weight (weight of the concentrated extract) to the initial weight (weight of the *A. thyrsiflora* powder used), and multiplying by 100% [39]. Therefore, the extract yield obtained was 19.1%. The ethanol extract yield met the requirements, as the standard for a concentrated extract yield is greater than 10%. Yield represents the percentage of the material remaining after extraction and serves to assess the effectiveness of the extraction [40].

3.2. Phytochemical Screening of *A. thyrsiflora* Leaves

Phytochemical screening was conducted for alkaloids, flavonoids, saponins, tannins, glycosides, and steroids using appropriate reagents. The results are shown in Table **1**.

Table 1. Phytochemical screening of ethanol extract of *A. thyrsiflora* leaves.

Sample	Compounds	Results
Ethanol extract of *A. thyrsiflora*	Alkaloids	+
	Flavonoids	+
	Saponins	+
	Tannins	+
	Glycosides	+
	Steroids	+

As shown in Table **1**, all phytochemical tests were positive for the six secondary metabolites. These positive results were indicated by changes in color, the formation of precipitates, and the development of foam. This is in line with the phytochemical screening of *A. thyrsiflora* leaves conducted by Marbun [41], who reported positive results for all secondary metabolites.

3.3. Biology Activity Prediction

The prediction of biological activity was performed on the PASS Online website, which displays the probability of activity (Pa) for each pharmacological effect that could occur in the compounds, as shown in Table **2**.

PASS Online is a database that predicts the activity spectrum of substances, which is used to predict the biological spectrum of compounds. If a compound has a bioactivity test value of Pa > 0.7, it has very high biological activity; if Pa < 0.5, the bioactivity is very low; and if 0.5 < Pa < 0.7, the bioactivity is moderate [42, 43]. According to that, 14 compounds fulfilled the requirement. Compounds that have good antineoplastic activity are 3',4'-dimethoxy-alpha-naphthoflavone; arbutin; 5-[6-hydroxy-5-(3-methylbut-2-enyl)-1-benzofuran-2-yl] benzene-1,3-diol; 4,4-Dimethyl-5 alpha-cholesta-8,14,24-trien-3 beta-ol; Myricetin; Mearnsitrin; Quercetin; Kaempferol. Compounds that have good Anticarcinogenic activity are (2S, 3S)-2, 3-Dihydro-2-[2-hydroxy-4-(beta-D-glucopyranosyloxy) phenyl]-3-(3, 5-dihydroxyphenyl) -4-[2-[4-(beta-D-glucopyranosyloxy) phenyl]ethenyl]benzofuran-6-ol; Myricetin; Mearnsitrin; Quercetin; Kaempferol; Isorhamnetin. In addition to the *Ampelocissus thyrsiflora*, some compounds have high antioxidant activity including 2S, 3S)-2, 3-Dihydro-2-[2-hydroxy-4-(beta-D-glucopyranosyloxy) phenyl]-3-(3, 5-dihydroxyphenyl) -4-[2-[4-(beta-D-glucopyranosyloxy) phenyl]ethenyl]benzofuran-6-ol; Myricetin; Mearnsitrin; Quercetin; Kaempferol; Isorhamnetin; DL-α-Tocopherol and apoptosis agonist are 3',4'-dimethoxy-alpha-naphthoflavone; 5-[6-hydroxy-5-(3-methylbut-2-enyl)-1-benzofuran-2-yl] benzene-1,3-diol; 4,4-Dimethyl-5 alpha-cholesta-8,14,24-trien-3 beta-ol; Myricetin; Quercetin; Kaempferol; α-Tocopherol. Apoptosis is essential for cell development and for maintaining the stable internal state (homeostasis) of tissues, including morphological changes [44]. Biological activities in the form of antineoplastic, apoptosis agonist, antioxidant, and anticarcinogen possessed by compounds in *A. thyrsiflora* Leaves indicate that this plant has the potential to be utilized in the treatment of breast cancer [45].

3.4. Physicochemical Prediction

The rule of five (ROF) is a parameter used to evaluate drug-likeness or to predict the potential pharmacological or biological activity of a chemical compound with oral activity as a medicine [46], as shown in Table **3**.

The description of + stands for requirements fulfilled, while – means requirements not fulfilled, physicochemical prediction results by Lipinski's Rule of Five of *A. thyrsiflora*. As has been written on Table **1**, 13 compounds that fulfilled Lipinski's Rule of Five are valproic acid; phenyl salicylate; ethylparaben; 3',4'-dimethoxy-alpha-naphthoflavone; dipropyleneglycol methyl ether acetate; 5-[6-hydroxy-5-(3-methylbut-2-enyl)-1-benzofuran-2-yl] benzene-1,3-diol; lauric acid; norethindrone acetate; 2, 4, 5-trihydroxy-7, 8-dioxonaphthalen-1 olate; kaempferol; isorhamnetin; hexadecanamide; 1-stearoylglycerol. A chemical compound is said to have good absorption or permeation if the Molar mass <500, the Number of H-bond acceptors <10, the Number of H-bond donors < 5, and Log *P* <5 [47]. If the compound has a molecular weight greater than 500 g/mol, it will be difficult to absorb and have low permeability [48].

Table 2. Biology activity prediction results by PASS online of *A. thyrsiflora*.

No.	Compound	Pa	Biological Activity
1	3',4'-dimethoxy-alpha-naphthoflavone	0,734	Antineoplastic
		0,743	Apoptosis agonist
2	Arbutin	0,829	Anti-carcinogenic
		0,782	Antioxidant
		0,787	Antineoplastic
3	5-[6-hydroxy-5-(3-methylbut-2-enyl)-1-benzofuran-2-yl] benzene-1,3-diol	0,718	Antineoplastic
		0,835	Apoptosis agonist
4	4,4-Dimethyl-5 alpha-cholesta-8,14,24-trien-3 beta-ol	0,746	Antineoplastic
		0,795	Apoptosis agonist
5	(2S, 3S)-2, 3-Dihydro-2-[2-hydroxy-4-(beta-D-glucopyranosyloxy)	0,881	Anti-carcinogenic
		0,723	Antioxidant
		0,781	Antineoplastic
6	[(2S,3R,4S,5S,6R)-3,4,5-trihydroxy-6-[[(2R,3R,4R,5R,6S)-3,4,5-trihydroxy-6-methyloxan-2-yl]oxymethyl]oxan-2-yl] (E)-3-phenylprop-2-enoate	0,865	Anti-carcinogenic
		0,736	Antioxidant
		0,861	Antineoplastic
7	Carthamoleusterone	0,781	Antineoplastic
8	Myricetin	0,784	Anti-carcinogenic
		0,924	Antioxidant
		0,841	Antineoplastic
		0,915	Apoptosis agonist
9	Mearnsitrin	0,952	Anti-carcinogenic
		0,898	Antioxidant
		0,878	Antineoplastic
		0,824	Apoptosis agonist
10	Quercetin	0,757	Anti-carcinogenic
		0,872	Antioxidant
		0,797	Antineoplastic
		0,887	Apoptosis agonist
11	Kaempferol	0,715	Anti-carcinogenic
		0,856	Antioxidant
		0,791	Antineoplastic
		0,881	Apoptosis agonist
12	5,8-dihydroxy-2-(4-hydroxyphenyl)-7-methoxy-3-{[(2S,3R,4R,5R,6S)-3,4,5-trihydroxy-6-methyloxan-2-yl]oxy}-4H-chrome-4-one	0,929	Anti-carcinogenic
		0,888	Antioxidant
		0,854	Antineoplastic
		0,803	Apoptosis agonist
13	Isorhamnetin	0,779	Anti-carcinogenic
		0,809	Antioxidant
		0,803	Antineoplastic
		0,88	Apoptosis agonist
14	DL-α-Tocopherol	0,967	Antioxidant
		0,736	Apoptosis agonist

Table 3. Physicochemical prediction results by Lipinski's Rule of Five of *A. thyrsiflora*.

No.	Compound	MW	Log P	HBD	HBA	Molar Refractivity	Desc.
1	Valproic Acid	144	2.28	1	2	40.94	+
2	Phenyl salicylate	214	2.61	1	3	59.5	+
3	Ribonic acid	166	-2.85	5	6	32.74	-
4	Ethylparaben	166	1.56	1	3	44.06	+
5	3',4'-dimethoxy-alpha-naphthoflavone	332	4.47	0	4	96.42	+
6	6,6,9-trimethyl-3-(3-methyl octan-2-yl)-7,8,9,10-tetrahydrobenzo[c]chromen-1-ol	370	7.45	1	2	114.46	-
7	Dipropylene glycol methyl ether acetate	190	0.98	0	4	48.51	+
8	Arbutin	272	-1.42	5	7	62.5	-
9	5-[6-hydroxy-5-(3-methylbut-2-enyl)-1-benzofuran-2-yl] benzene-1,3-diol	310	4.53	3	4	89.11	+
10	Lauric acid	200	3.99	1	2	59.47	+
11	4,4-Dimethyl-5 alpha-cholesta-8,14,24-trien-3 beta-ol	410	8	1	1	128.23	-
12	Norethindrone acetate	340	4.06	0	3	95.42	+
13	2, 4, 5-trihydroxy-7, 8-dioxonaphthalen-1-olate	221	0	3	6	49.61	+
14	(2S, 3S)-2, 3-Dihydro-2-[2-hydroxy-4-(beta-D-glucopyranosyloxy) phenyl]-3-(3, 5-dihydroxyphenyl) -4-[2-[4-(beta-D-glucopyranosyloxy) phenyl]ethenyl]benzofuran-6-ol	752	-3.46	0	17	162.78	-
15	3-hydroxy-3 methyl butanoate	118	0.23	2	3	28.55	-
16	Acetic acid	60	0.09	1	2	13.3	-
17	1-Naphthylbis (9-anthryl) methylation	493	6.44	0	0	150.04	-
18	4-phenylethynylnaphthalic anhydride	526	7.78	0	3	162.48	-
19	[(2S,3R,4S,5S,6R)-3,4,5-trihydroxy-6-[[(2R,3R,4R,5R,6S)-3,4,5-trihydroxy-6-methyloxan-2-yl]oxymethyl]oxan-2-yl] (E)-3-phenylprop-2-enoate	456	-2.1	6	11	106.55	-
20	ethane	30	1.02	0	0	11.34	-
21	(13Z, 16Z)-docosa-13, 16-dienoic acid	336	7.44	1	2	105.46	-
22	Carthamoleusterone	508	3.99	4	8	136.32	-
23	5-propan-2-yl-1, 3-benzodioxole	696	8.31	0	7	192.14	-
24	3-[(2-carboxyacetyl) oxymethoxy]-3-oxopropanoic acid	220	-1.02	2	8	41.55	-
25	Myricetin	318	1.71	6	8	75.71	-
26	Mearnsitrin	478	0.3	7	12	111.41	-
27	Quercetin	302	2.01	5	7	74.05	-
28	Kaempferol	286	2.3	4	6	72.38	+
29	5,8-dihydroxy-2-(4-hydroxyphenyl)-7-methoxy-3-{[(2S,3R,4R,5R,6S)-3,4,5-trihydroxy-6-methyloxan-2-yl]oxy}-4H-chrome-4-one	440	-1.32	0	11	92.07	-
30	Isorhamnetin	316	2.31	4	7	78.93	+
31	Oleamide	281	5.5	2	2	88.64	-
32	Hexadecanamide	255	4.95	2	2	79.5	+
33	Stearamide	283	5.73	2	2	88.74	-
34	1-Stearoylglycerol	358	4.5	3	4	103.65	+
35	Tridemorph	297	5.4	0	2	92.9	-
36	Erucamide	337	7.06	2	2	107.11	-
37	Bis(2-ethylhexyl) phthalate	390	6.2	0	4	112.68	-
38	Stearic acid	337	7.06	2	2	107.11	-
39	DL-α-Tocopherol	430	8.84	1	2	134.39	-

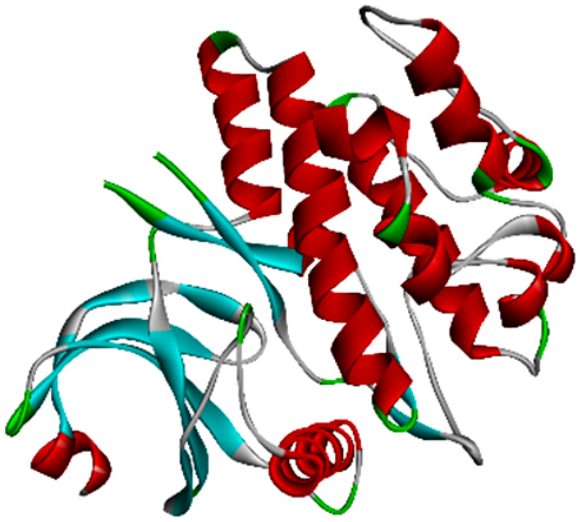

Fig. (1). Structure of WEE1 after receptor preparation.

3.5. Receptor Preparation and Docking Validation

Protein used for this study is WEE1 (PDB ID: 5VC5), homo sapiens organism, resolution value 1.93 Å, which can be seen in Fig. (**1**).

3.6. Docking Validation

The RMSD (Root Mean Square Deviation) value for WEE1 was 1.195 Å, indicating that the docking results were valid, as the RMSD value was below the accepted threshold of 2.0 Å [49] (Fig. **2**). The prepared receptors were then docked with ligands using AutoDock Vina to obtain amino acid residues, binding affinities, and standard deviations.

3.7. Docking Result with Biovia Discovery Studio

Biovia Discovery Studio visualized the biomolecular interactions, allowing researchers to analyze the interactions and bonds created between ligand and protein in the binding pockets. Table **4** reports the mean binding affinity as the average of two binding affinity measurements per compound, since each was conducted twice.

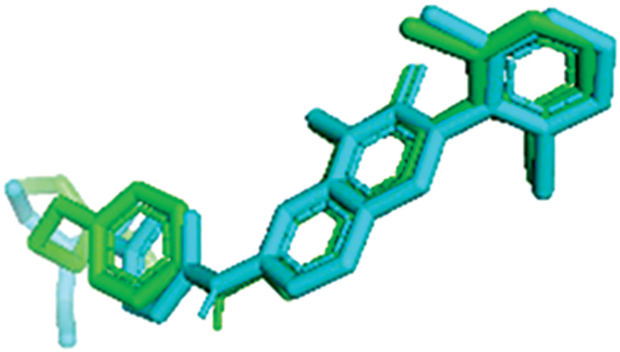

Fig. (2). The validation result of the native ligand (green) and ligand docking (blue) of WEE1.

Table 4. Molecular docking results of *A. thyrsiflora* to WEE1.

No.	Compounds	H-Bond Interaction	Hydrophobic Bond Interaction	Binding Affinity
1	Adavosertib	PHE310, GLU377, ASP463	ILE305, VAL313, ALA326, LYS328, VAL360, PHE433	-10.09 ± 0.38
2	Native ligand	GLU377, CYS379	ILE305, VAL313, ALA326, LYS328, ASP386	-9.54 ± 0.24
3	Valproic Acid	LYS331	PHE310	-3.48 ± 0.28
4	Phenyl salicylate	-	ALA326, LYS328, ILE374, CYS379, PHE433	-7.65 ± 0.07
5	Ribonic acid	MET425, ASP426, LEU483	-	-5.73 ± 0.1
6	Ethylparaben	-	ALA326, VAL360, CYS379, PHE433	-6.11 ± 0.01
7	3',4'-dimethoxy-alpha-naphthoflavone	GLY306, SER307, ASN376	ILE305, VAL313, ALA326	-9.03 ± 0.0
8	6,6,9-trimethyl-3-(3-methyloctan-2-yl)-7,8,9,10-tetrahydrobenzo[c]chromen-1-ol	SER307, GLU309	GLY308, PHE310	-2.53 ± 0.57
9	Dipropylene glycol methyl ether acetate	PHE310, LYS328, LYS331	-	-4.09 ± 0.09
10	Arbutin	SER307, SER312, ARG329	-	-4.96 ± 0.15
11	5-[6-hydroxy-5-(3-methylbut-2-enyl)-1-benzofuran-2-yl] benzene-1,3-diol	PRO333	PHE310, LYS331, ASP339. HIS466	-7.22 ± 0.0
12	Lauric acid	LYS328	ILE305, VAL313, ALA326, VAL360, CYS 379, PHE433	-5.77 ± 0.09
13	4,4-Dimethyl-5 alpha-cholesta-8,14,24-trien-3 beta-ol	-	PHE314	-6.25 ± 0.48
14	Norethindrone acetate	-	PHE310, LYS331	-6.08 ± 0.26
15	2, 4, 5-trihydroxy-7, 8-dioxonaphthalen-1-olate	PHE310, LYS331	GLU309, ASP339	-6.39 ± 0.58

(Table 4) contd.....

No.	Compounds	H-Bond Interaction	Hydrophobic Bond Interaction	Binding Affinity
16	(2S, 3S)-2, 3-Dihydro-2-[2-hydroxy-4-(beta-D-glucopyranosyloxy) phenyl]-3-(3, 5-dihydroxyphenyl) -4-[2-[4-(beta-D-glucopyranosyloxy) phenyl]ethenyl]benzofuran-6-ol	LYS304, SER307, GLU309, SER312, ARG329	GLY308, PHE310	-6.89 ± 0.16
17	3-hydroxy-3-methyl butanoate	SER307, GLY308, GLY311	-	-1.94 ± 0.18
18	Acetic acid	GLU309	-	-0.98 ± 0.0
19	1-Naphthylbis (9-anthryl) methylcation	-	VAL338	-2.77 ± 0.05
20	4-phenylethynylnaphthalic anhydride	-	VAL338	-2.58 ± 0.02
21	[(2S,3R,4S,5S,6R)-3,4,5-trihydroxy-6-[[(2R,3R,4R,5R,6S)-3,4,5-trihydroxy-6-methyloxan-2-yl]oxymethyl]oxan-2-yl] (E)-3-phenylprop-2-enoate	GLY308, GLU309, LYS328, ASP463	PHE310, VAL313, PRO333, ASP339	-6.39 ± 0.58
22	Ethane	-	PHE310	-1.41 ± 0.0
23	(13Z, 16Z)-docosa-13, 16-dienoic acid	SER312, ARG329	-	-3.72 ± 0.0
24	Carthamoleusterone	PHE310	-	-1.68 ± 0.39
25	5-propan-2-yl-1, 3-benzodioxole	-	ARG329	-3.88 ± 0.0
26	3-[(2-carboxyacetyl) oxymethoxy]-3-oxopropanoic acid	LYS304, GLY311, SER312, ARG329, HIS371	-	-4.45 ± 0.1
27	Myricetin	PHE310, ALA343	ASP339	-6.46 ± 0.0
28	Mearnsitrin	LYS331	LYS304	-5.94 ± 0.61
29	Quercetin	ASP 339	GLU309, PHE310, ASP339	-6.7 ± 0.0
30	Kaempferol	PHE310, LYS328, LYS331	PRO333, ASP339	-6.55 ± 0.23
31	5,8-dihydroxy-2-(4-hydroxyphenyl)-7-methoxy-3-{[(2S,3R,4R,5R,6S)-3,4,5-trihydroxy-6-methyloxan-2-yl]oxy}-4H-chromen-4-one	PHE310, LYS328, PRO333, LEU334, SER337, ASP339	GLU309	-7.13 ± 0.19
32	Isorhamnetin	PHE310, ASP426, LYS428	ASP339, HIS466	-6.46 ± 0.01
33	Oleamide	SER312, ARG329	PHE310	0.8 ± 1.63
34	Hexadecanamide	SER307, SER312	PHE310	-2.81 ± 0.23
35	Stearamide	SER304, SER312	PHE314	-1.69 ± 0.15
36	1-Stearoylglycerol	GLY308, GLY311	PHE314	-2.97 ± 0.06
37	Tridemorph	GLY308	PHE310, PHE314	-2.38 ± 0.24
38	Erucamide	ASP339	VAL338	-2.17 ± 0.03
39	Bis(2-ethylhexyl) phthalate	-	PHE310, VAL338, ASP339	-2.03 ± 0.09
40	Stearic acid	ASP339	VAL338	-1.64 ± 0.14
41	DL-α-Tocopherol	-	PHE310	-3.84 ± 0.65

Binding affinity is a value that indicates the accuracy of the bond between the ligand and the target protein [50]. The lower the binding affinity, the stronger the bond between the ligand and the receptor, making it a promising therapeutic candidate [51]. The binding affinity of the WEE1 protein ranged from 0.8 to -10.09. The standard drug, Adavosertib, and native ligand (96M) exhibit the lowest binding affinity.

Based on previous research, the binding modes between WEE1 and WEE1 inhibitors include the pyrimidine nitrogen adjacent to an amino group forming H-bonds with the CYS379 backbone, hydroxyl groups on the pyridine side chain forming H-bonds with ASP463, and the pyrazolopyridinone core establishing π-stacking interactions with PHE433 [52]. Other hydrogen bonds that contribute to inhibitory activity have been reported with ILE305, LYS328, and ASP339 [53-55]. In our docking results, several compounds interacted with the same critical amino acid residues within the WEE1 binding pocket. Among them, four compounds: kaempferol,

myricetin, quercetin, and isorhamnetin were prioritized not only because they displayed relatively favorable binding affinities, but also because they consistently engaged key residues known to be essential for WEE1 inhibition [56]. Importantly, affinity does not necessarily predict activity, as binding ligands may behave as either agonists or competitive inhibitors depending on their interactions within the active site. Therefore, the quality and specificity of amino acid interactions play a crucial role in determining whether a ligand truly disrupts the biological function of the target protein [57]. This dual criterion of binding strength and residue-specific interactions provided a strong rationale for selecting these four flavonoids for subsequent molecular dynamics simulations over 100 ns to further evaluate their stability and binding modes.

3.8. Molecular Dynamics Simulations

Molecular dynamics simulations were done using GROMACS and CHARMM-GUI for input file preparation. MD simulations were performed for a 100 ns trajectory. The visualization of the ligand throughout the 100 ns simulations can be seen in Fig. (**3**).

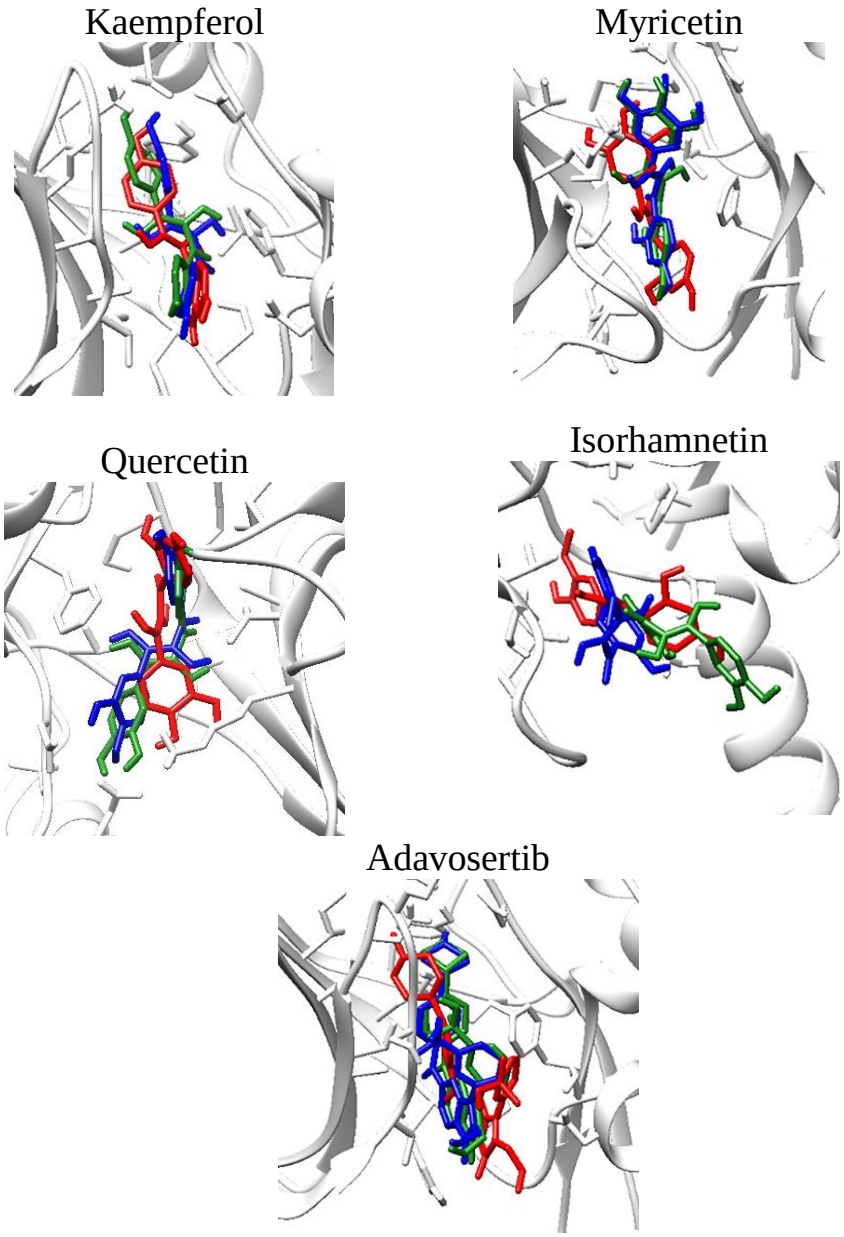

Fig. (3). Visualization of the WEE1-ligand complexes throughout the 100 ns simulations, red (0 ns), green (50 ns), blue (100 ns).

From the visualization above, it can be seen that the ligand stays in the binding site throughout the 100 ns simulation. Analysis of the RMSD, RMSF, SASA, and Hydrogen bonds formed during the simulations was also done. The results are shown in Fig. (**4**).

RMSD is an atom's average movement or displacement at a specific time interval that provides data on the average distance between ligands and proteins. Based on the results, the RMSD of the WEE1-ligand complex shows a slight increase at 0.5 ns, followed by greater stability thereafter. The interaction between ligand-receptor is considered stable if the RMSD value is under 2.5 nm, in which these results show a stable interaction [58, 59].

Root-mean-square fluctuation (RMSF) aims to evaluate the mobility of molecular systems. The RMSF value measures the degree of structural flexibility or rigidity of individual atoms within a molecule or system [60]. The RMSF data show that the fluctuations of the WEE1-ligands happen between 0.03 and 0.5 nm, with the activation segment peaking in 370 to 410 residues. The fluctuation in the activation segment indicates the ability to bind ligands and elicit a biological response; these results align with findings that the WEE1 binding pocket involves ASN 376, GLU 377, CYS 379, and ASP 386 [52]. A high RMSF value indicates a flexible region, while a low RMSF value indicates the rigidity of the amino acid [61, 62].

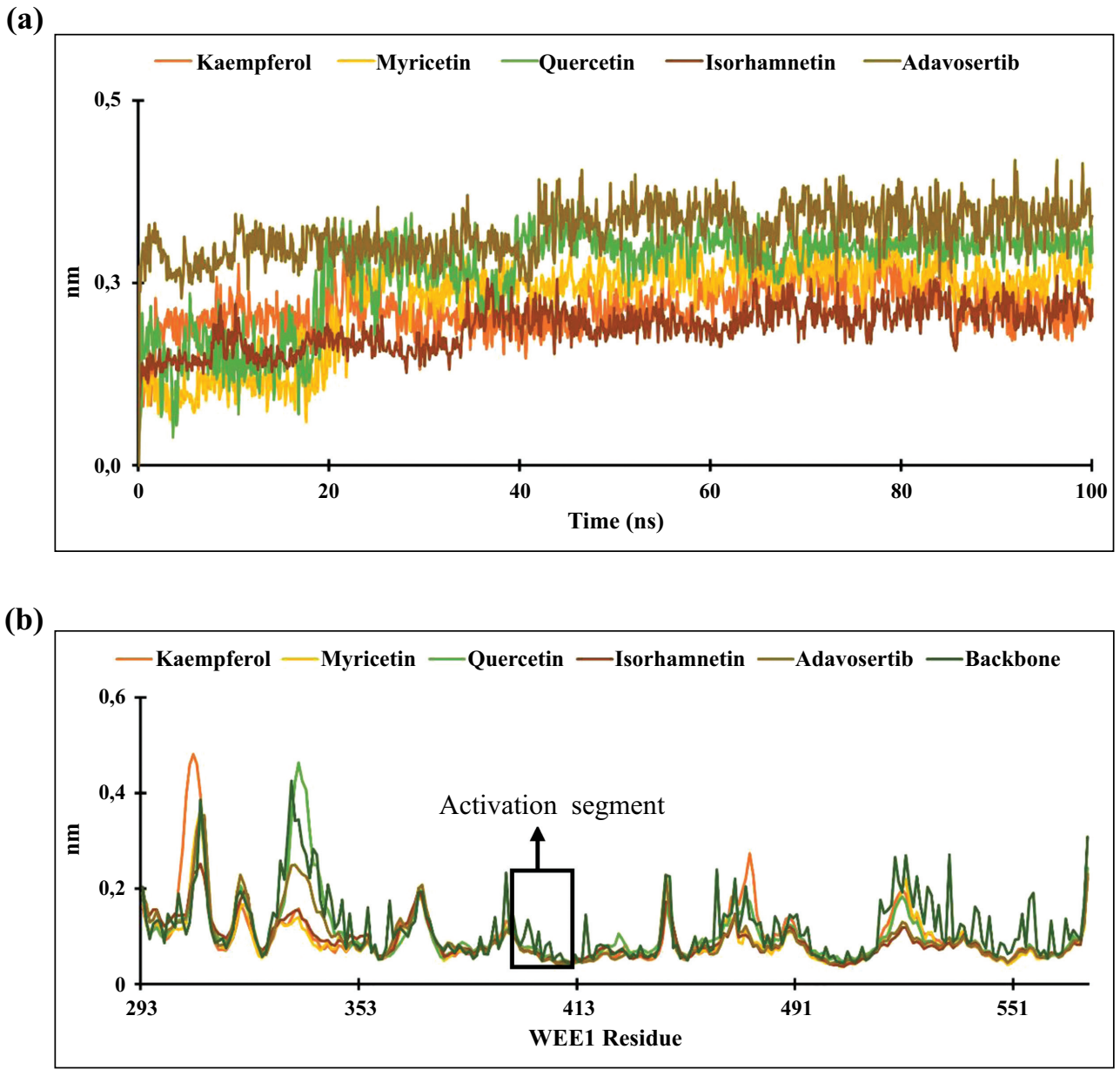

Fig. 4 contd.....

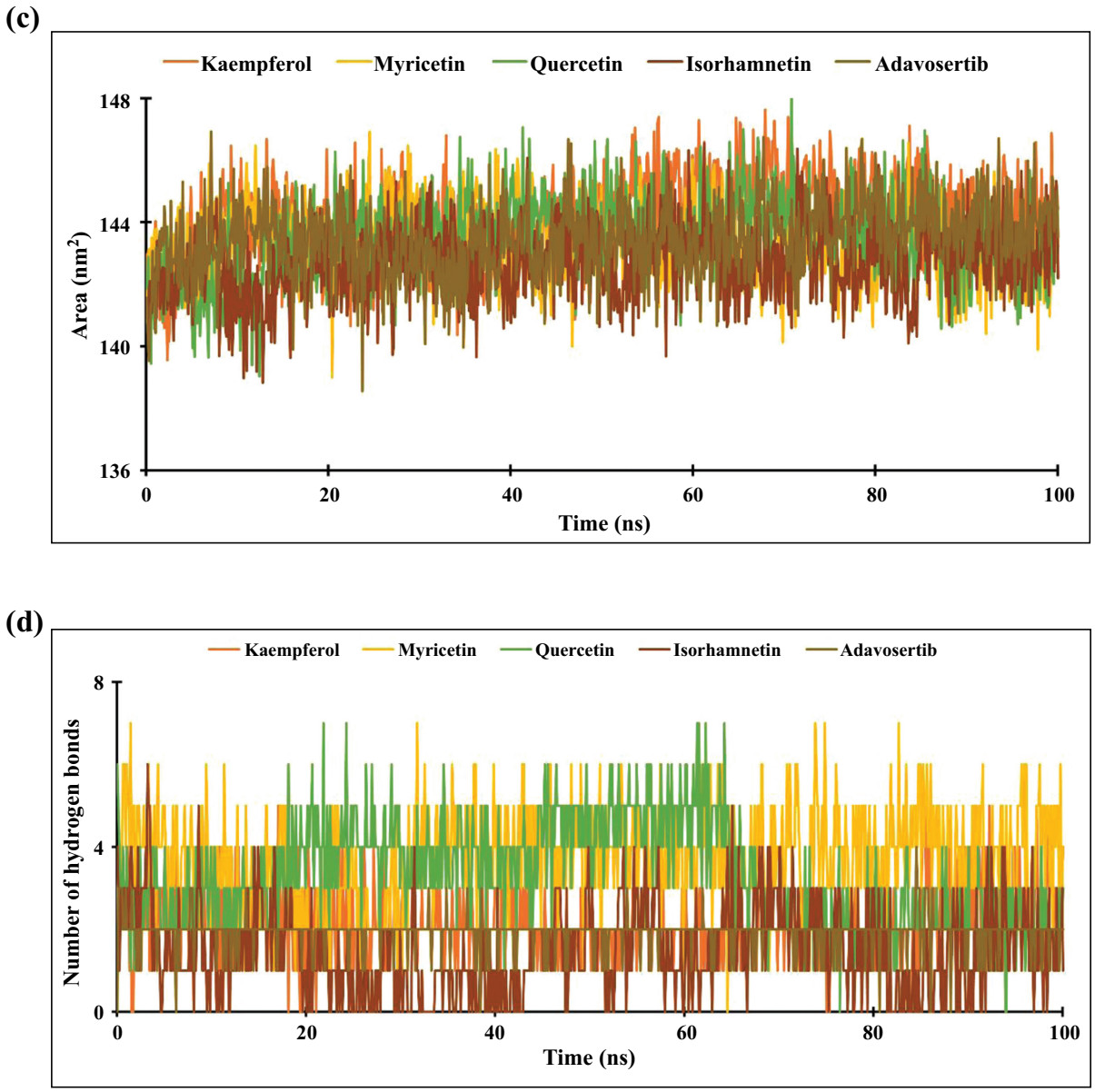

Fig. (4). Analysis of the (**a**) RMSD of WEE1-ligand complex; (**b**) RMSF of WEE1-ligand complex; (**c**) SASA of WEE1-ligand complex; (**d**) hydrogen bond of WEE1-ligand complex.

The solvent-accessible surface area (SASA) is the surface area of a molecule that can come into contact with the solvent [63]. From the results, the SASA of the ligand-receptor complexes remained stable throughout the simulations, ranging from 138 to 148 nm2. Higher SASA values indicate larger, looser proteins and more flexible protein conformations, which correlate with increased interaction potential with other molecules, such as ligands [64].

Hydrogen bonding is an interaction that occurs in hydrogen atoms contained in a pair of other atoms that have an affinity for electrons [65]. The ligand will remain close to the protein-binding site through permanent hydrogen bonds [61]. In the results, the number of hydrogen bonds formed during the simulation ranged from 0 to 7 for WEE-ligand complexes.

Further analysis was done to obtain each complex's amino acid residues and MMPBSA value. The results are shown in Table **5**.

MMPBSA analysis was then done to estimate ligand-binding affinities. Evdw (Van der Waals energy) accounts for the weak intermolecular forces and significantly contributes to the overall binding free energy. Electrostatic energy (Eele) plays a crucial role initially but often cancels out the polar solvation energy due to the solvent's screening effect. Epolar (Polarsolvation energy)

represents the electrostatic interactions between the solute and the surrounding solvent. Enon-polar (Nonpolar solvation energy) encompasses the effects of creating a cavity in the solvent and the subsequent solvent rearrangement around the solute [66-68]. The total energy is summed from the components to produce each component's average total free energy. So, to calculate the binding free energy, the total free energy of the receptor and ligand is subtracted from the total free energy of the complex [69]. The results demonstrated that kaempferol, myricetin, and quercetin exhibited lower binding free energies than the standard drug adavosertib, indicating stronger binding affinities for the WEE1 receptor. These flavonoids are widely recognized for their anticancer activities, with numerous reports describing their ability to induce apoptosis, inhibit proliferation, and modulate signaling pathways in breast cancer cells. Notably, quercetin has previously been reported to inhibit WEE1 activity, supporting the credibility of our computational predictions [17]. Both quercetin and the other flavonoids formed key interactions with critical WEE1 amino acid residues, including hydrogen bonds with GLU377 and CYS379, as well as hydrophobic interactions with ALA326 and CYS379, which are known to contribute to WEE1 inhibition [52]. To validate these computational findings, an *in vitro* cytotoxicity assay using the MTT method was conducted on the MCF-7 breast cancer cell line. The combined *in silico* and *in vitro* results suggest that the metabolite compounds present in *A. thyrsiflora* leaves have promising potential as WEE1 inhibitors, warranting further investigation.

3.9. Cytotoxicity Assay

The cytotoxicity result of the ethanol extract of *A. thyrsiflora* leaves against MCF-7 cell lines can be seen in Fig. (**5**) and Table **6**.

Table 5. Amino acid residues and MMPBSA of WEE1-ligand complex.

Compounds	Amino Acid Residue		MMPBSA				
	H-bond Interaction	Hydrophobic Bonds Interaction	ΔE_{VDW}	ΔE_{ELE}	ΔE_{polar}	$\Delta E_{non\ polar}$	ΔE_{GTOTAL}
Kaempferol	LYS328, ASN376, GLU377, CYS379	VAL313, ALA326, CYS379	-36.90 ± 0.42	-35.16 ± 0.95	46.88 ± 0.96	-4.93 ± 1.00	-30.11 ± 0.57
Myricetin	GLU377, CYS379	ALA326, CYS379	-38.31 ± 0.57	-48.41 ± 0.55	59.58 ± 0.51	-5.79 ± 0.09	-32.93 ± 0.71
Isorhamnetin	GLY308, ASP386	ILE305	-25.79 ± 0.31	-21.33 ± 0.08	36.98 ± 0.14	-4.13 ± 0.06	-14.27 ± 0.30
Quercetin	GLU346, GLU377, CYS379, GLY382	ILE305, VAL313, ALA326, LYS328, PHE433	-36.11 ± 0.04	-36.43 ± 0.31	49.94 ± 0.07	-5.35 ± 0.08	-27.95 ± 0.43
Adavosertib	ASN376, GLU377, TYR378, CYS379	ILE305, VAL313, ALA326, VAL360, CYS379, PHE433	-45.85 ± 0.07	-29.18 ± 0.05	59.14 ± 0.07	-6.43 ± 0.33	-22.31 ± 0.27

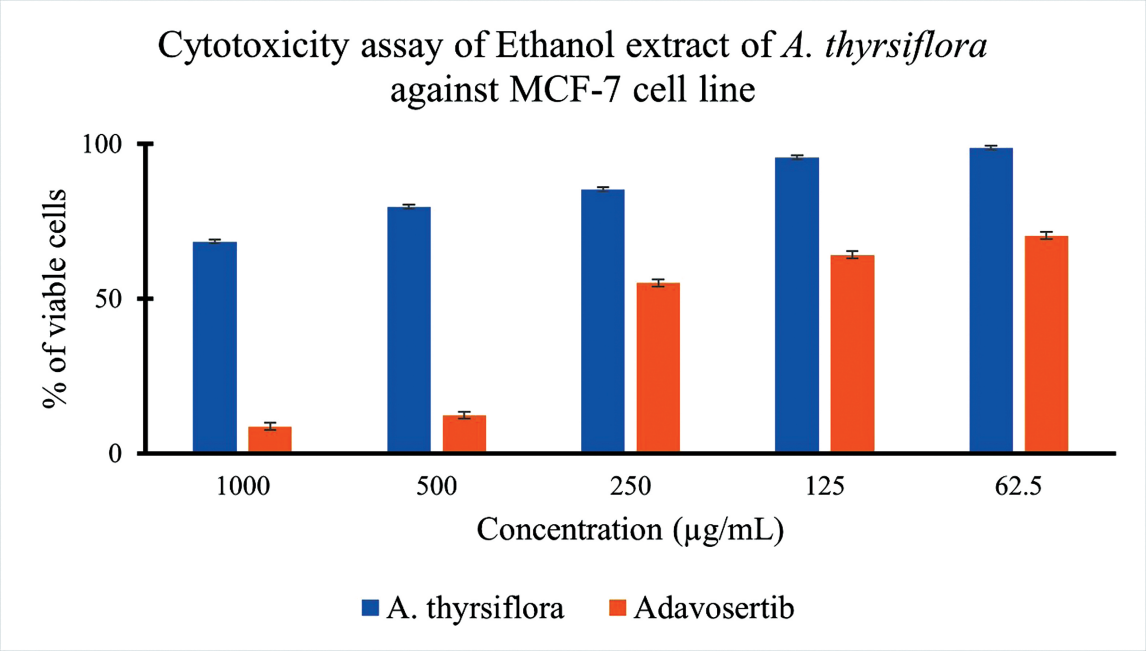

Fig. (5). % of viable cells of ethanol extract of *A. thyrsiflora* and Adavosertib treatment against the MCF-7 cell line.

Table 6. IC_{50} value of cytotoxicity assay to the MCF-7 cell line.

Value	Ethanol Extract of *A. thyrsiflora*	Adavosertib
IC_{50} (µg/ml)	2011.25 ± 42.71	175.98 ± 1.66

The MTT assay is based on the ability of mitochondrial dehydrogenases, primarily succinate dehydrogenase in metabolically active cells, to reduce the yellow tetrazolium salt, MTT (3-(4,5-dimethylthiazol-2-yl)-2,5-diphenyltetrazolium bromide), into insoluble purple formazan crystals. Since only viable cells with intact mitochondria and cell membranes can perform this reduction, the amount of formazan formed is directly proportional to the number of living cells and can be quantified using a spectrophotometer [70, 71]. In addition to determining cytotoxic effects, the MTT assay provides the half-maximal inhibitory concentration (IC_{50}), which is a standard parameter used to evaluate the potency of cytotoxic agents in cell-based assays [72]. As shown above, cell viability decreased with increasing extract concentration. At 1000 µg/mL of the ethanol extract of *A. thyrsiflora*, cell viability dropped to 68%, whereas treatment with 1000 µg/mL of Adavosertib reduced cell viability by 91%. Adavosertib is a well-known WEE1 inhibitor with an IC_{50} of 175.98 ± 1.66 µg/mL, and its activity is associated with disruption of the G2/M checkpoint, inhibition of DNA damage repair, and induction of apoptosis [73]. The calculated IC_{50} value indicated that the extract exhibited limited cytotoxic activity, according to the classification criteria set by the U.S. National Cancer Institute [74]. Although the ethanol extract of *A. thyrsiflora* demonstrated a high IC50 value, the observed dose-dependent decrease in MCF-7 cell viability suggests the presence of bioactive constituents with potential anticancer effects. In particular, the potential cytotoxic activity may be attributed to secondary metabolites within the extract, such as alkaloids, flavonoids, and saponins, which are widely reported to exert cytotoxic effects on breast cancer cells [75-77]. Additional assays, including proliferation inhibition and apoptosis induction, are warranted to fully characterize the extract's therapeutic potential against breast cancer cells.

4. LIMITATIONS OF THIS STUDY

This study has several limitations that should be acknowledged. The *in silico* analyses were performed under simplified conditions that may not fully represent the biological environment. The *in vitro* evaluation was conducted on a single breast cancer cell line, MCF-7, which may limit the generalizability of the cytotoxicity results. Future studies involving multiple cell lines, mechanistic assays, and *in vivo* validation would strengthen and expand these findings.

CONCLUSION

WEE1 is a key regulator of the cell cycle and a potential therapeutic target, especially for breast cancer therapy. The ethanol extract of *Ampelocissus thyrsiflora* was found to contain flavonoids, glycosides, and steroids, known for their anticancer potential. Although some compounds did not meet physicochemical criteria, molecular docking and dynamics simulations were performed to explore their interactions with the WEE1 receptor. Of the 39 compounds identified, three demonstrated strong and stable interactions with WEE1, supported by favorable binding affinities and low MM-PBSA energy values. These compounds formed key hydrogen bonds with GLU 377 and CYS 379, and hydrophobic interactions with ALA 326 and CYS 379, residues critical for WEE1 inhibition. To support these findings, an *in vitro* MTT assay in MCF-7 cells confirmed a dose-dependent cytotoxic effect. Nonetheless, the combined *in silico* and *in vitro* results suggest that *A. thyrsiflora* metabolites hold promise as early-stage WEE1 inhibitors and merit further investigation.

AUTHORS' CONTRIBUTIONS

The authors confirm contribution to the paper as follows: H.S.W.: Study conception and design; N.: Data collection; S.Y.: Analysis and interpretation of results; G.T.: Visualization; P.B.N.: Investigation; C.C.J.: Draft manuscript. All authors reviewed the results and approved the final version of the manuscript.

LIST OF ABBREVIATIONS

GCO	=	Global Cancer Observatory
CDK1	=	Cyclin Dependent-Kinase 1
DNA	=	Deoxyribonucleic Acid
BSLT	=	Brine Shrimp Lethality Test
SIRT1	=	Sirtuin1
AMPK	=	AMP-Activated Protein Kinase
MTT	=	3-[4,5-dimethylthiazol-2-yl]-2,5 diphenyl tetrazolium bromide
SMILES	=	Simplified Molecular Input Line Entry System
MD	=	Molecular Dynamics
RMSD	=	Root Mean Square Deviation
RMSF	=	Root Mean Square Fluctuation
SASA	=	Solvent Accessible Surface Area
MMPBSA	=	Molecular Mechanics Poisson-Boltzmann Surface Area

ETHICAL STATEMENT

Ethical approval was obtained from the Animal Research Ethics Committee of the Faculty of Mathematics and Natural Sciences, Universitas Sumatera Utara, Indonesia (Approval No. 0950/KEPH-FMIPA/2024).

CONSENT FOR PUBLICATION

Not applicable.

AVAILABILITY OF DATA AND MATERIALS

The data and supportive information are available within the article.

FUNDING

The authors would like to thank the TALENTA Research Program, Universitas Sumatera Utara, Indonesia for funding this research through research contract No. 18589/UN5.1.R/PPM/2024, dated 30 May 2024.

CONFLICT OF INTEREST

The authors declare no conflict of interest, financial or otherwise.

ACKNOWLEDGEMENTS

The authors would like to thank the Faculty of Pharmacy, Universitas Sumatera, and the Faculty of Medicine, Public Health, and Nursing, Universitas Gadjah Mada, Indonesia for their assistance and support, and for facilitating the study.

REFERENCES

[1] Saini, A.; Kumar, M.; Bhatt, S.; Saini, V.; Malik, A. Cancer causes and treatments. *Int. J. Pharm. Sci. Res.,* **2020**, *11*(7), 3121-3134. http://dx.doi.org/10.13040/ijpsr.0975-8232.11(7).3109-22

[2] Huang, J.; Chan, P.S.F.; Lok, V.; Chen, X.; Ding, H.; Jin, Y.; Yuan, J.; Lao, X.; Zheng, Z.J.; Wong, M.C.S. Global incidence and mortality of breast cancer: A trend analysis. *Aging,* **2021**, *13*(4), 5748-5803. http://dx.doi.org/10.18632/aging.202502 PMID: 33592581

[3] Cancer today. **2022**. Available from: https://gco.iarc.fr/today/en

[4] Rohani, A.S.; Wahyuni, H.S.; Putra, E.D.; Nazliniwaty; Auletta, C.; Rasyida, T. Computational investigation of the inhibition of CHK1 and WEE1 proteins by chemical constituents of Amaranthus gangeticus. *Int. J. Appl. Pharm.,* **2025**, *17*, 481-487. http://dx.doi.org/10.22159/ijap.2025v17i5.53996

[5] Zhang, Z.; Harish, R.; Elahi, N.; Saini, S.; Telia, A.; Kundlas, M.; Koroleva, A.; Umoh, I.N.; Lota, M.; Bilkhu, M.; Kawaiah, A.; Allala, M.R.; Leukeu, A.; Nebuwa, E.; Sharifi, N.; Ashton, A.W.; Jiao, X.; Pestell, R.G. Targeting WEE1 kinase for breast cancer therapeutics: An update. *Int. J. Mol. Sci.,* **2025**, *26*(12), 5701-5724. http://dx.doi.org/10.3390/ijms26125701 PMID: 40565165

[6] Esposito, F.; Giuffrida, R.; Raciti, G.; Puglisi, C.; Forte, S. Wee1 Kinase: A potential target to overcome tumor resistance to therapy. *Int. J. Mol. Sci.,* **2021**, *22*(19), 10689-10712. http://dx.doi.org/10.3390/ijms221910689 PMID: 34639030

[7] Wani, T.A.; Zargar, S.; Hussain, A. Spectroscopic, thermodynamic and molecular docking studies on molecular mechanisms of drug binding to proteins. *Molecules,* **2022**, *27*(23), 8405-8410. http://dx.doi.org/10.3390/molecules27238405 PMID: 36500497

[8] Teo, Z.L.; O'Connor, M.J.; Versaci, S.; Clarke, K.A.; Brown, E.R.; Percy, L.W.; Kuykhoven, K.; Mintoff, C.P.; Savas, P.; Virassamy, B.; Luen, S.J.; Byrne, A.; Sant, S.; Lindeman, G.J.; Darcy, P.K.; Loi, S. Combined PARP and WEE1 inhibition triggers anti-tumor immune response in BRCA1/2 wildtype triple-negative breast cancer. *NPJ Breast Cancer,* **2023**, *9*(1), 68-83. http://dx.doi.org/10.1038/s41523-023-00568-5 PMID: 37582853

[9] Roering, P.; Siddiqui, A.; Heuser, V.D.; Potdar, S.; Mikkonen, P.; Oikkonen, J.; Li, Y.; Pikkusaari, S.; Wennerberg, K.; Hynninen, J.; Grenman, S.; Huhtinen, K.; Auranen, A.; Carpén, O.; Kaipio, K. Effects of Wee1 inhibitor adavosertib on patient-derived high-grade serous ovarian cancer cells are multiple and independent of homologous recombination status. *Front. Oncol.,* **2022**, *12*, 954430-954443. http://dx.doi.org/10.3389/fonc.2022.954430 PMID: 36081565

[10] Cole, K.A.; Ijaz, H.; Surrey, L.F.; Santi, M.; Liu, X.; Minard, C.G.; Maris, J.M.; Voss, S.; Reid, J.M.; Fox, E.; Weigel, B.J. Pediatric phase 2 trial of a WEE1 inhibitor, adavosertib (AZD1775), and irinotecan for relapsed neuroblastoma, medulloblastoma, and rhabdomyosarcoma. *Cancer,* **2023**, *129*(14), 2245-2255. http://dx.doi.org/10.1002/cncr.34786 PMID: 37081608

[11] van den Boogaard, W.M.C.; Komninos, D.S.J.; Vermeij, W.P. Chemotherapy side-effects: Not all DNA damage is equal. *Cancers,* **2022**, *14*(3), 627-655. http://dx.doi.org/10.3390/cancers14030627 PMID: 35158895

[12] Midoen, Y.H.; Ilyas, S.; Santoso, P.; Situmorang, P.C. Effect of maximal physical exercise on apoptosis *via* cytochrome c in hippocampus cells after administration of *Vitis gracilis* Wall. *J. Pharm. Pharmacogn. Res.,* **2023**, *11*(2), 297-307. http://dx.doi.org/10.56499/jppres22.1563_11.2.297

[13] Wasnis, N.Z.; Ilyas, S.; Hutahaean, S.; Silaban, R.; Situmorang, P.C. Effect of *Vitis gracilis* Wall (*gagatan harimau*) in the recovery of gastrocnemius muscle cells and cytochrome c expression of Mus musculus. *J. Pharm. Pharmacogn. Res.,* **2022**, *10*(2), 303-309. http://dx.doi.org/10.56499/jppres21.1208_10.2.303

[14] Wasnis, N.; Ilyas, S.; Hutahaean, S.; Silaban, R.; Situmorang, P. Analysis of Apoptotic Cells and Lung Inflammation after Given by *Vitis gracilis*. *Pak. J. Biol. Sci.,* **2022**, *25*(11), 1033-1039. http://dx.doi.org/10.3923/pjbs.2022.1033.1039 PMID: 36591935

[15] Midoen, Y.H.; Ilyas, S.; Santoso, P. Assessing the hepatoprotective efficacy of *Vitis gracilis* Wall. against doxorubicin-induced hepatic injury in rats. *J. Pharm. Pharmacogn. Res.,* **2024**, *12*(6), 1178-1186. http://dx.doi.org/10.56499/jppres24.1983_12.6.1178

[16] Surbakti, C.; Nasution, L.R.; Rudang, S.N.; Cintya, H.; Vany, I.; Agnes, P.A.T.; Elsa, S.E.S. Toxicity test of ethanol extract of *gagatan harimau* leaves (*Vitis gracilis* B.L.) on Artemia salina Leach larvae using brine shrimp lethal test (BSLT) method. *Int. J. Sci. Technol. Manag.,* **2023**, *4*, 1501-1505. http://dx.doi.org/10.46729/ijstm.v4i6.963

[17] Santoso, P; Ilyas, S; Midoen, YH; Maliza, R; Belahusna, DF Predictive bioactivity of compounds from *Vitis gracilis* leaf extract to counteract doxorubicin-induced cardiotoxicity *via* sirtuin 1 and adenosine monophosphate-activated protein kinase: An *in-silico* study. *J Appl Pharm Sci*, **2024**, *14*(4), 099-114. http://dx.doi.org/10.7324/JAPS.2024.167007

[18] Rana, J. N.; Gul, K.; Mumtaz, S. Isorhamnetin: Reviewing recent developments in anticancer mechanisms and nanoformulation-driven delivery. *Int. J. Mol. Sci.,* **2025**, *26*(15), 7381-7381. http://dx.doi.org/10.3390/ijms26157381 PMID: 40806510

[19] Wang, Q.; Chen, Y.; Lu, H.; Wang, H.; Feng, H.; Xu, J.; Zhang, B. Quercetin radiosensitizes non-small cell lung cancer cells through the regulation of miR-16-5p/WEE1 axis. *IUBMB Life,* **2020**, *72*(5), 1012-1022. http://dx.doi.org/10.1002/iub.2242 PMID: 32027086

[20] Benjamin, I.; Udoikono, A.D.; Louis, H.; Agwamba, E.C.; Unimuke, T.O.; Owen, A.E.; Adeyinka, A.S. Antimalarial potential of naphthalene-sulfonic acid derivatives: Molecular electronic properties, vibrational assignments, and *in-silico* molecular docking studies. *J. Mol. Struct.,* **2022**, *1264*, 133298-133312. http://dx.doi.org/10.1016/j.molstruc.2022.133298

[21] Systemes, D. Biovia Discovery Studio. **2016**. Available from: https://discover.3ds.com/discovery-studio-visualizer-download

[22] Arsyad, R.; Amin, A.; Waris, R. The technique of manufacture and values of simplicia and ethanol extract of bagore (caesalpinia crista l.) seeds original polewali mandar. *MNPJ,* **2023**, *1*, 138-147. http://dx.doi.org/10.33096/mnpj.v1i3.47

[23] Vásquez Salazar, E.E.; Hernández, G.R.; Vargas Saavedra, J.A.; Villegas Romero, H.J. Ethanol extraction desalination test using pre-treated mine wastewater concentrated by reverse osmosis. *Desalination Water Treat.,* **2024**, *317*, 100208-100216. http://dx.doi.org/10.1016/j.dwt.2024.100208

[24] Zulfiah, Herman Uji identifikasi senyawa alkaloid ekstrak metanol daun kelor (Moringa Oleifera Lamk) menggunakan metode metode Kromatografi Lapis Tipis. *J Farm Sandi Karsa,* **2020**, *6*, 83-87.
http://dx.doi.org/10.36060/jfs.v6i2.75

[25] Dubale, S.; Kebebe, D.; Zeynudin, A.; Abdissa, N.; Suleman, S. Phytochemical screening and antimicrobial activity evaluation of selected medicinal plants in Ethiopia. *J. Exp. Pharmacol.,* **2023**, *15*, 51-62.
http://dx.doi.org/10.2147/JEP.S379805 PMID: 36789235

[26] Sabdoningrum, E.K.; Hidanah, S.; Chusniati, S. Characterization and phytochemical screening of Meniran (Phyllanthus niruri Linn) extract's nanoparticles used ball mill method. *Pharmacogn. J.,* **2021**, *13*(6s), 1568-1572.
http://dx.doi.org/10.5530/pj.2021.13.200

[27] Filimonov, D.A.; Lagunin, A.A.; Gloriozova, T.A.; Rudik, A.V.; Druzhilovskii, D.S.; Pogodin, P.V.; Poroikov, V.V. Prediction of the biological activity spectra of organic compounds using the PASS online web resource. *Chem. Heterocycl. Compd.,* **2014**, *50*(3), 444-457.
http://dx.doi.org/10.1007/s10593-014-1496-1

[28] Lipinski, C.A. Lead- and drug-like compounds: The rule-of-five revolution. *Drug Discov. Today. Technol.,* **2004**, *1*(4), 337-341.
http://dx.doi.org/10.1016/j.ddtec.2004.11.007 PMID: 24981612

[29] Eberhardt, J.; Santos-Martins, D.; Tillack, A.F.; Forli, S. AutoDock Vina 1.2.0: New docking methods, expanded force field, and python bindings. *J. Chem. Inf. Model.,* **2021**, *61*(8), 3891-3898.
http://dx.doi.org/10.1021/acs.jcim.1c00203 PMID: 34278794

[30] Mao, T.; Chen, B.; Wei, W.; Chen, G.; Liu, Z.; Wu, L.; Li, X.; Pathak, J.L.; Li, J. AutoDock and molecular dynamics-based therapeutic potential prediction of flavonoids for primary Sjögren's syndrome. *Heliyon,* **2024**, *10*(13), 33860.
http://dx.doi.org/10.1016/j.heliyon.2024.e33860 PMID: 39027572

[31] Ahmad Usmani, S.; Ishaq, S.; Habib, O.; Tahir, R.; Rahman, S.U.; Sarwar, S.; Ajmal Khan, M.; Ahmad, A.; Aziz, A.; Ullah, A. Computational analysis of variant in tyrosinase protein using molecular dynamic simulation: An *in silico* approach. *Results Chem.,* **2024**, *11*, 101779-101792.
http://dx.doi.org/10.1016/j.rechem.2024.101779

[32] Yekeen, A.A.; Durojaye, O.A.; Idris, M.O.; Muritala, H.F.; Arise, R.O. CHAPERON*g*: A tool for automated GROMACS-based molecular dynamics simulations and trajectory analyses. *Comput. Struct. Biotechnol. J.,* **2023**, *21*, 4849-4858.
http://dx.doi.org/10.1016/j.csbj.2023.09.024 PMID: 37854635

[33] Kognole, A.A.; Lee, J.; Park, S.J.; Jo, S.; Chatterjee, P.; Lemkul, J.A.; Huang, J.; MacKerell, A.D., Jr; Im, W. CHARMM-GUI Drude prepper for molecular dynamics simulation using the classical Drude polarizable force field. *J. Comput. Chem.,* **2022**, *43*(5), 359-375.
http://dx.doi.org/10.1002/jcc.26795 PMID: 34874077

[34] Park, S.J.; Kern, N.; Brown, T.; Lee, J.; Im, W. CHARMM-GUI PDB manipulator: Various PDB structural modifications for biomolecular modeling and simulation. *J. Mol. Biol.,* **2023**, *435*(14), 167995-168002.
http://dx.doi.org/10.1016/j.jmb.2023.167995 PMID: 37356910

[35] Protokol. **2009**. Available from: https://ccrc.farmasi.ugm.ac.id/protokol/

[36] Senthilraja, P.; Kathiresan, K. *In vitro* cytotoxicity MTT assay in Vero, HepG2 and MCF -7 cell lines study of Marine Yeast. *J. Appl. Pharm. Sci.,* **2015**, *5*, 080-084.
http://dx.doi.org/10.7324/JAPS.2015.50313

[37] Cao, S.; Liang, J.; Chen, M.; Xu, C.; Wang, X.; Qiu, L.; Zhao, X.; Hu, W. Comparative analysis of extraction technologies for plant extracts and absolutes. *Front Chem.,* **2025**, *13*, 1536590-1536605.
http://dx.doi.org/10.3389/fchem.2025.1536590 PMID: 40099208

[38] Saerang, F.; Edy, H.J.; Siampa, J.P. Formulation of cream with ethanol extract of green gedi leaf (Abelmoschus Manihot L.) against Propionibacterium acnes. *Pharmakon,* **2023**, *12*, 350-357.
http://dx.doi.org/10.35799/pha.12.2023.49075

[39] Xiao, J.; Wu, J.; Chao, Y.; Liu, R.; Li, C.; Xiao, Z. Evaluation of yields and quality parameters of oils from Cornus wilsoniana fruit extracted by subcritical n-butane extraction and conventional methods. *Grain Oil Sci. Technol.,* **2022**, *5*(4), 204-212.
http://dx.doi.org/10.1016/j.gaost.2022.09.003

[40] Senduk, TW; Montolalu, LADY; Dotulong, V The rendement of boiled water extract of mature leaves of mangrove Sonneratia alba. *J. Perikanan Kelaut. Trop.,* **2020**, *11*, 9-15.
http://dx.doi.org/10.35800/jpkt.11.1.2020.28659

[41] Surbakti, C.; Siallagan, A.F.; Lubis, M.F.; Nasution, L.R. Optimization microwave-assisted extraction (MAE) to obtain total phenol from *Ampelocissus thyrsiflora* (Blume) Planch leaves for antibacterial activity response of *Staphylococcus Epidermidis*. *Multidisciplinary Science Journal,* **2025**, *7*(9), 2025423.
http://dx.doi.org/10.31893/multiscience.2025423

[42] Filimonov, D.A.; Rudik, A.V.; Dmitriev, A.V.; Poroikov, V.V. Computer-aided estimation of biological activity profiles of drug-like compounds taking into account their metabolism in human body. *Int. J. Mol. Sci.,* **2020**, *21*(20), 7492-7504.
http://dx.doi.org/10.3390/ijms21207492 PMID: 33050610

[43] Shamna, J.J.; Jose, J.; Shijikumar; Ahmed, R. A brief study of nephrotoxicity and nephroprotective agents. *Indian J Pharm Biol Res.,* **2020**, *8*(1), 09-13.
http://dx.doi.org/10.30750/ijpbr.8.1.2

[44] Abdullah, M.L.; Al-Shabanah, O.; Hassan, Z.K.; Hafez, M.M. Eugenol-induced autophagy and apoptosis in breast cancer cells *via* PI3K/AKT/FOXO3a pathway inhibition. *Int. J. Mol. Sci.,* **2021**, *22*(17), 9243-9259.
http://dx.doi.org/10.3390/ijms22179243 PMID: 34502165

[45] Shuja, N.; Ansari, M.A.; Phull, Q.Z.; Sodhar, J.M.; Shuja, A.; Maqsood, M. Antineoplastic mechanism of emblica officinalis against breast cancer, A humans clinical cross sectional study. *Pak. J. Med. Health Sci.,* **2022**, *16*(2), 502-504.
http://dx.doi.org/10.53350/pjmhs22162502

[46] Ivanović, V.; Rančić, M.; Arsić, B.; Pavlović, A. Lipinski's rule of five, famous extensions and famous exceptions. *Chemia Naissensis,* **2020**, *3*(1), 171-181.
http://dx.doi.org/10.46793/ChemN3.1.171I

[47] Wilapangga, A.; Sutyono, B.; Permadi, T.; Noordam, E.R. Potensi Farmakokinetika dan Toksisitas Benzyl β-D-Glucoside dari Piper crocatum: Studi *in silico*. *J Syifa Sci Clin Res.,* **2024**, *6*(2), 173-180.
http://dx.doi.org/10.37311/jsscr.v6i2.27054

[48] Yeni, Y.; Rachmania, R.A. The prediction of pharmacokinetic properties of compounds in *Hemigraphis alternata* (Burm. F.) T. ander leaves using pkCSM. *Indones J Chem.,* **2022**, *22*(4), 1081-1089.
http://dx.doi.org/10.22146/ijc.73117

[49] Shamsian, S.; Sokouti, B.; Dastmalchi, S. Benchmarking different docking protocols for predicting the binding poses of ligands complexed with cyclooxygenase enzymes and screening chemical libraries. *Bioimpacts,* **2023**, *14*(2), 29955-29965.
http://dx.doi.org/10.34172/bi.2023.29955 PMID: 38505677

[50] Jones, D.; Kim, H.; Zhang, X.; Zemla, A.; Stevenson, G.; Bennett, W.F.D.; Kirshner, D.; Wong, S.E.; Lightstone, F.C.; Allen, J.E. Improved protein-ligand binding affinity prediction with structure-based deep fusion inference. *J. Chem. Inf. Model.,* **2021**, *61*(4), 1583-1592.
http://dx.doi.org/10.1021/acs.jcim.0c01306 PMID: 33754707

[51] Ru, X.; Ye, X.; Sakurai, T.; Zou, Q. NerLTR-DTA: Drug–target binding affinity prediction based on neighbor relationship and learning to rank. *Bioinformatics,* **2022**, *38*(7), 1964-1971.
http://dx.doi.org/10.1093/bioinformatics/btac048 PMID: 35134828

[52] Du, X.; Li, J.; Luo, X.; Li, R.; Li, F.; Zhang, Y.; Shi, J.; He, J. Structure-activity relationships of Wee1 inhibitors: A review. *Eur. J. Med. Chem.,* **2020**, *203*, 112524-112539.
http://dx.doi.org/10.1016/j.ejmech.2020.112524 PMID: 32688199

[53] Hu, Y.; Zhou, L.; Zhu, X.; Dai, D.; Bao, Y.; Qiu, Y. Pharmacophore

modeling, multiple docking, and molecular dynamics studies on Wee1 kinase inhibitors. *J. Biomol. Struct. Dyn.,* **2019**, *37*(10), 2703-2715. http://dx.doi.org/10.1080/07391102.2018.1495576 PMID: 30052133

[54] Li, Y.; Wu, D.; Kong, L.; Zhang, S.; Du, H.; Sun, W.; Zhang, L.; Li, Y.; Zuo, Z. Ensemble docking-based virtual screening toward identifying inhibitors against Wee1 kinase. *Future Med. Chem.,* **2019**, *11*(15), 1889-1906. http://dx.doi.org/10.4155/fmc-2019-0022 PMID: 31517534

[55] Jin, T.; Xu, W.; Chen, R.; Shen, L.; Gao, J.; Xu, L.; Chi, X.; Lin, N.; Zhou, L.; Shen, Z.; Zhang, B. Discovery of potential WEE1 inhibitors *via* hybrid virtual screening. *Front. Pharmacol.,* **2023**, *14*, 1298245-1298256. http://dx.doi.org/10.3389/fphar.2023.1298245 PMID: 38143493

[56] Ouassaf, M.; Mazri, R.; Khan, S.U.; Rengasamy, K.R.R.; Alhatlani, B.Y. Machine learning-guided screening and molecular docking for proposing naturally derived drug candidates against MERS-CoV 3CL protease. *Int. J. Mol. Sci.,* **2025**, *26*(7), 3047-3047. http://dx.doi.org/10.3390/ijms26073047 PMID: 40243651

[57] Rowaiye, A. B.; Oni, S.; Uzochukwu, I. C.; Akpa, A.; Esimone, C. O. Structure-based virtual screening for natural compounds that bind with the activating receptors of natural killer cells. *bioRxiv,* **2020**, *1*, 1-34. http://dx.doi.org/10.1101/2020.06.19.160861

[58] Manandhar, S.; Sankhe, R.; Priya, K.; Hari, G.; Kumar B, H.; Mehta, C.H.; Nayak, U.Y.; Pai, K.S.R. Molecular dynamics and structure-based virtual screening and identification of natural compounds as Wnt signaling modulators: Possible therapeutics for Alzheimer's disease. *Mol. Divers.,* **2022**, *26*(5), 2793-2811. http://dx.doi.org/10.1007/s11030-022-10395-8 PMID: 35146638

[59] Mirzadeh, A.; Kobakhidze, G.; Vuillemot, R.; Jonic, S.; Rouiller, I. *In silico* prediction, characterization, docking studies and molecular dynamics simulation of human p97 in complex with p37 cofactor. *BMC Mol. Cell Biol.,* **2022**, *23*(1), 39. http://dx.doi.org/10.1186/s12860-022-00437-2 PMID: 36088301

[60] Fatriansyah, J.F.; Rizqillah, R.K.; Yandi, M.Y.; Fadilah; Sahlan, M. Molecular docking and dynamics studies on propolis sulabiroin-A as a potential inhibitor of SARS-CoV-2. *J. King Saud Univ. Sci.,* **2022**, *34*(1), 101707-101716. http://dx.doi.org/10.1016/j.jksus.2021.101707 PMID: 34803333

[61] Fatriansyah, J.F.; Boanerges, A.G.; Kurnianto, S.R.; Pradana, A.F.; Fadilah; Surip, S.N. Molecular dynamics simulation of ligands from *Anredera cordifolia* (Binahong) to the main protease (Mpro) of SARS-CoV-2. *J. Trop. Med.,* **2022**, *2022*, 1-13. http://dx.doi.org/10.1155/2022/1178228 PMID: 36457332

[62] Khedraoui, M.; Nour, H.; Yamari, I.; Abchir, O.; Errougui, A.; Chtita, S. Design of a new potent Alzheimer's disease inhibitor based on QSAR, molecular docking and molecular dynamics investigations. *Chemical Physics Impact,* **2023**, *7*, 100361-100372. http://dx.doi.org/10.1016/j.chphi.2023.100361

[63] Peng, S.; Wang, Z.; Yu, P.; Liao, G.; Liu, R.; Wang, D.; Zhang, W. Aggregation and construction mechanisms of microbial extracellular polymeric substances with the presence of different multivalent cations: Molecular dynamic simulation and experimental verification. *Water Res.,* **2023**, *232*, 119675-119683. http://dx.doi.org/10.1016/j.watres.2023.119675 PMID: 36758351

[64] Xie, J.; Shi, Y.; Luo, W.; Fang, W.; Luo, L.; Zeng, L. Effects of theacrine on the astringency of EGCG by affecting salivary protein − EGCG interactions through different molecular mechanisms. *Food Chem. X,* **2024**, *22*, 101474-101482. http://dx.doi.org/10.1016/j.fochx.2024.101474 PMID: 38817981

[65] Yusuff, OK; Omotosho, K; Raji, AT Comparative chains dynamics of triosephosphate isomerase investigated by molecular dynamics simulation. *J. Chem. Soc. Niger.,* **2023**, *48*, 146-153. http://dx.doi.org/10.46602/jcsn.v48i1.856

[66] Genheden, S.; Ryde, U. The MM/PBSA and MM/GBSA methods to estimate ligand-binding affinities. *Informa Healthcare,* **2015**, *10*, 450-454. http://dx.doi.org/10.1517/17460441.2015.1032936

[67] Cavani, M.; Riofrío, W.A.; Arciniega, M. Molecular dynamics and MM-PBSA analysis of the SARS-CoV-2 gamma variant in complex with the hACE-2 receptor. *Molecules,* **2022**, *27*(7), 2370-2385. http://dx.doi.org/10.3390/molecules27072370 PMID: 35408761

[68] Damayanti, M.M.; Rachmawati, M.; Widiyastuti, E.; Kharisma, Y.; Fakih, T.M.; Arfan, A.; Ramadhan, D.S.F. Structure-based design through molecular dynamics approaches of the small-molecule bioactive compounds in cinnamon as interleukin 6 (IL-6) inhibitors. *Rasayan J. Chem.,* **2022**, *2022*, 158-166. http://dx.doi.org/10.31788/RJC.2022.1558192

[69] Hassab, M.A.E.; Fares, M.; Amin, M.K.A.H.; Al-Rashood, S.T.; Alharbi, A.; Eskandrani, R.O.; Alkahtani, H.M.; Eldehna, W.M. Toward the identification of potential α-ketoamide covalent inhibitors for SARS-CoV-2 main protease: Fragment-based drug design and MM-PBSA calculations. *Processes,* **2021**, *9*(6), 1004-1017. http://dx.doi.org/10.3390/pr9061004

[70] Rai, Y.; Pathak, R.; Kumari, N.; Sah, D.K.; Pandey, S.; Kalra, N.; Soni, R.; Dwarakanath, B.S.; Bhatt, A.N. Mitochondrial biogenesis and metabolic hyperactivation limits the application of MTT assay in the estimation of radiation induced growth inhibition. *Sci. Rep.,* **2018**, *8*(1), 1531-1545. http://dx.doi.org/10.1038/s41598-018-19930-w PMID: 29367754

[71] Vajrabhaya, L.; Korsuwannawong, S. Cytotoxicity evaluation of a Thai herb using tetrazolium (MTT) and sulforhodamine B (SRB) assays. *J. Anal. Sci. Technol.,* **2018**, *9*(1), 15-20. http://dx.doi.org/10.1186/s40543-018-0146-0

[72] Larsson, P.; Engqvist, H.; Biermann, J.; Werner Rönnerman, E.; Forssell-Aronsson, E.; Kovács, A.; Karlsson, P.; Helou, K.; Parris, T.Z. Optimization of cell viability assays to improve replicability and reproducibility of cancer drug sensitivity screens. *Sci. Rep.,* **2020**, *10*(1), 5798-5809. http://dx.doi.org/10.1038/s41598-020-62848-5 PMID: 32242081

[73] Ariyoshi, M.; Yuge, R.; Kitadai, Y.; Shimizu, D.; Miyamoto, R.; Yamashita, K.; Hiyama, Y.; Takigawa, H.; Urabe, Y.; Oka, S. WEE1 inhibitor adavosertib exerts antitumor effects on colorectal cancer, especially in cases with *p53* mutations. *Cancers,* **2024**, *16*(18), 3136-3155. http://dx.doi.org/10.3390/cancers16183136 PMID: 39335109

[74] Widiandani, T.; Tandian, T.; Zufar, B.D.; Suryadi, A.; Purwanto, B.T.; Hardjono, S.; Siswandono, S. *In vitro* study of pinostrobin propionate and pinostrobin butyrate: Cytotoxic activity against breast cancer cell T47D and its selectivity index. *J. Public Health Africa,* **2023**, *14*(1), 6. http://dx.doi.org/10.4081/jphia.2023.2516 PMID: 37492547

[75] Elekofehinti, O.O.; Iwaloye, O.; Olawale, F.; Ariyo, E.O. Saponins in cancer treatment: Current progress and future prospects. *Pathophysiology,* **2021**, *28*(2), 250-272. http://dx.doi.org/10.3390/pathophysiology28020017 PMID: 35366261

[76] Rampogu, S.; Balasubramaniyam, T.; Lee, J.H. Phytotherapeutic applications of alkaloids in treating breast cancer. *Biomed. Pharmacother.,* **2022**, *155*, 113760-113775. http://dx.doi.org/10.1016/j.biopha.2022.113760 PMID: 36271547

[77] Zasheva, D.; Mladenov, P.; Zapryanova, S.; Gospodinova, Z.; Georgieva, M.; Alexandar, I.; Velinov, V.; Djilianov, D.; Moyankova, D.; Simova-Stoilova, L. Cytotoxic effects of plant secondary metabolites and naturally occurring bioactive peptides on breast cancer model systems: Molecular mechanisms. *Molecules,* **2024**, *29*(22), 5275-5297. http://dx.doi.org/10.3390/molecules29225275 PMID: 39598664